A comparative study of the scattering of highly energetic atomic and molecular beams from metallic surfaces

Massimo F. Bertino,[a] J. R. Manson,[b] and W. Silvestri
Max-Planck-Institut für Strömungsforschung, Bunsenstrasse 10, D-37073 Göttingen, Germany

(Received 5 January 1998; accepted 19 March 1998)

Time-of-flight spectra (TOF) of supersonic He and D_2 beams in the energy range $100 \leqslant E_i \leqslant 250$ meV have been measured after scattering from a clean Cu(001) surface at surface temperatures between 100 and 950 K. The TOF spectra of both He and D_2 exhibit broad featureless distributions over the whole range of incident beam energies and surface temperatures. The intensities of the He TOF spectra are a factor of 5 to 7 higher than those of D_2 when the incident beam energies are the same and below 200 meV. For the highest incident beam energies $E_i \geqslant 200$ meV and surface temperatures $T_s > 700$ K the difference between the He and D_2 TOF spectra reduces to about a factor of 3. A theoretical model is employed which reproduces the TOF spectra to a very good approximation. The comparison of the best-fit parameters for He and D_2 provides valuable information on the interaction parameters and their dependence on incident energy. The analysis of the energy and temperature dependence of the peak intensities of the D_2 TOF spectra allows for the separation of the contribution of rotational excitations in the collision mechanism.
 [S0021-9606(98)01424-X]

I. INTRODUCTION

During the last ten years scattering of thermal beams of He atoms from surfaces has become established as one of the more powerful techniques of surface science. Most measurements have concentrated on the quantum features of the interaction of He with surfaces, that is diffraction and single-phonon inelastic measurements of He beams with incident energy $E_i \approx 50$ meV. The regime of high-incident energies and surface temperatures has been rarely investigated experimentally[1] because of the onset of multiphonon effects which complicate the analysis of the experimental data. Only very recently has theoretical and experimental work analyzed systematically He scattering from metallic surfaces in the multiphonon regime.[2–11] These studies concentrated on the transition between the single-phonon quantum regime and the multiphonon classical regime and showed that theory and experiment are in good agreement for incident beam energies $E_i \leqslant 120$ meV.

In this work time-of-flight (TOF) measurements of highly energetic He and D_2 beams scattered from a Cu(001) surface are reported. The incident beam energy E_i was varied between 100 and 250 meV and the surface temperature T_s was between 100 and 950 K. The measurements presented in this article are the first systematic study of He and D_2 scattering in the true multiphonon classical regime and allow a direct, energy-resolved comparison between scattering from the same surface of atoms and molecules with the same mass. Due to the innovative character of this investigation, the Cu(001) surface represents an ideal candidate because of its simplicity and because of the good results obtained by previous investigations with He beams in both the quantum and the multiphonon scattering regimes.[2–5,12]

This paper is organized as follows. In Sec. II the essential elements of the theory of multiphonon scattering are described. In Sec. III the experimental technique is described, while the experimental results are presented in Sec. IV and discussed in Sec. V.

II. THEORY

In general, gas–surface collision phenomena can be divided into two regimes. At low incident energies and surface temperatures (typically $E_i < 70$ meV and $T_s < 500$ K for many low-index metallic surfaces) single quantum energy exchanges predominate and result in sharp peaks in both TOF spectra and angular distributions. At high incident energies and surface temperatures the classical multiphonon regime predominates and both TOF spectra and angular distributions become broad and featureless.[4,5]

A well-established criterion to discriminate between the two regimes is given by the Debye–Waller exponent $2W$. The expression for the Debye–Waller exponent is given by

$$W(T_s) = \frac{3\hbar^2(\mathbf{k}_f' - \mathbf{k}_i')^2 T_s}{2M k_B \Theta_D^2}. \tag{1}$$

In Eq. (1) M is the mass of a surface atom, $\mathbf{k}_f'$ and $\mathbf{k}_f'$ are the incident and scattered wave vectors (where the prime denotes the Beeby correction in which the perpendicular components include the physisorption well depth[13]) of the incident and scattered wave vectors, T_s is the surface temperature, Θ_D is the Debye temperature of the surface and k_B is the Boltzmann constant. The single quantum regime is expected when $2W \leqslant 1$ and the classical multiphonon regime for $2W \geqslant 6$.[14] In this experiment the Debye exponent varies

[a]Permanent address: Department of Chemistry, Massachusetts Institute of Technology, Cambridge, Massachusetts 02139.
[b]Permanent address: Department of Physics and Astronomy, Clemson University, Clemson, South Carolina 29634.

for He scattering from a minimum value $2W_{\min}(\mathrm{He})\sim 1.5$ at $T_s=100$ K and $E_i=105$ meV to a maximum value $2W_{\max}(\mathrm{He})\sim 30$ at $T_s=950$ K and $E_i=253$ meV when a surface Debye temperature $\Theta_D=270$ K and a potential well depth $\epsilon=5.76$ meV are assumed.[15,16] In the case of D_2 scattering for the present experimental conditions the Debye exponent varies from a minimum value $2W_{\min}(D_2)\sim 4$ at $T_s=100$ K and $E_i=101$ meV to a maximum value $2W_{\max}(D_2)\sim 70$ at $T_s=950$ K and $E_i=251$ meV when a value $\epsilon=32.5$ meV for the potential well depth is assumed.[17] The experimental conditions are therefore almost always in the multiphonon classical regime for both He and D_2 scattering.

A complete formal theory of the many-body scattering quantum problem has been derived by one of the authors[14] with use of classical trajectories. This theory will be referred to as the ''full quantum theory'' in the following. Under the extreme semiclassical assumptions of scattering from a continuum surface at high energies and at large surface temperatures (for which $2W\geqslant 6$) a differential reflection coefficient can be analytically calculated which expresses the fraction of particles scattered into the final energy interval dE_f and solid angle $d\Omega_f$. This differential reflection coefficient is[14,18]

$$\frac{dR}{d\Omega_f\, dE_f}=\frac{m^2|\mathbf{k}_f|v_R^2}{4\pi^3\hbar^5 k_{iz}S_{\mathrm{u.c.}}}\,|\tau_{fi}|^2\left(\frac{\hbar^2\pi}{\Delta E_0 k_B T_s}\right)^{3/2}\times\exp\left\{-\frac{(\Delta E+\Delta E_0)^2+2\hbar^2 v_R^2\Delta K^2}{4k_B T_s\Delta E_0}\right\}, \quad (2)$$

where $S_{\mathrm{u.c.}}$ is the area of the surface unit cell, $\Delta\mathbf{K}=\mathbf{K}_f-\mathbf{K}_i$ is the surface parallel component of the wave vector transfer, and v_R is a weighted average of surface phonon velocities parallel to the surface. Here ΔE_0 is the classical recoil energy and is equivalent to the energy given up to the surface if the incoming projectile were colliding with a single, initially stationary surface atom. This is expressed by the relation

$$\Delta E_0=\frac{\hbar^2(\mathbf{k}_f-\mathbf{k}_i)^2}{2M}. \quad (3)$$

The factor $|\tau_{fi}|^2$ in Eq. (2) is a form factor which can be expressed in terms of a cutoff function in parallel momentum $\Delta\mathbf{K}$ and the Mott–Jackson matrix element of the one-dimensional potential $v(z)=\exp(-\beta z)$,[19–21]

$$|\tau_{fi}|^2=\exp\left(-\frac{\Delta K^2}{Q_c^2}\right)\left(\frac{\hbar^2\beta^2}{4\pi m}\right)^2 pq\,\sinh(p)\sinh(q)\times\left[\frac{p^2-q^2}{(\cosh(p)-\cosh(q))^2}\right]^2, \quad (4)$$

where $p=2\pi k'_{iz}/\beta$, $q=2\pi k'_{fz}/\beta$, and Q_c is the cutoff parameter.[21,22]

For the comparisons with experiment considered below it is useful to discuss the general characteristics of Eq. (2), in particular the characteristic signatures such as the peak position, maximum intensity, and the full width at half maximum (FWHM). The intensity at the point of most probable energy transfer is dictated by the prefactor envelope function of Eq. (2) and its value goes as

$$I_{\mathrm{MAX}}\propto\frac{1}{(k_B T_s\Delta E_0)^{3/2}}. \quad (5)$$

However, if the interaction potential were given by a target of discrete scattering centers the intensity at the most probable energy transfer has a weaker dependence on E_i and T_s given by[8,18,23]

$$I_{\mathrm{MAX}}\propto\frac{1}{(k_B T_s\Delta E_0)^{1/2}}. \quad (6)$$

The characteristic power law exponent provides a clear signature difference between the two extreme limits. Recent measurements[4,12] have shown, however, that the intensities of the TOF spectra for He scattering in the multiphonon regime have a dependence on T_s which varies very nearly as $T_s^{-3/2}$ as predicted by Eq. (2).

The width of the energy distribution is dictated by two factors, the semiclassical form factor $|\tau_{fi}|^2$ of Eq. (4) and the Gaussian-type exponential of Eq. (2). Under special circumstances, such as when E_f and E_i are of widely different magnitude or for the case of large mass ratios between the projectile and target atoms, the exponential in Eq. (2) becomes highly skewed because of the energy dependence of ΔE_0. Since under the present experimental conditions the intensity is very much Gaussian in shape, the temperature dependence of the FWHM is given essentially by the Gaussian-type exponential of Eq. (2) and it is relatively straightforward to extract its behavior. Ignoring the term in $\Delta\mathbf{K}^2$ and expanding the argument of the exponent of Eq. (2) about the point $\Delta E+\Delta E_0=0$ produces a FWHM which can be expressed as

$$(\mathrm{FWHM})^2\approx 16\ln(2)g(\theta)E_i k_B T_s, \quad (7)$$

where $\Delta E+\Delta E_0=0$ is equivalent to the kinematical expression of Baule for the position of the energy loss peak as a function of angle in a binary collision between the projectile and a single stationary surface atom given by[19,24]

$$E_f=f(\theta)E_i, \quad (8)$$

where

$$f(\theta)=\left(\frac{\sqrt{1-\mu^2\sin^2\theta}+\mu\cos\theta}{1+\mu}\right)^2. \quad (9)$$

Here, $\mu=m/M$ is the mass ratio and θ is the total scattering angle, which for the present experiment is $\theta=\pi-\theta_f-\theta_i$. The function $g(\theta)$ appearing in Eq. (7) is then given by

$$g(\theta)=\frac{g_{\mathrm{TA}}(\theta)}{(1+\mu-\mu\cos\theta/\sqrt{f(\theta)})^2} \quad (10)$$

and

$$g_{\mathrm{TA}}(\theta)=\mu(1+f(\theta)-2\sqrt{f(\theta)}\cos\theta) \quad (11)$$

is the value taken by $g(\theta)$ in the trajectory approximation (TA). The trajectory approximation is obtained upon assuming that the recoil energy shift ΔE_0 appearing in the argument of the exponential in Eq. (2) is constant, in which case

$$\langle(\mathrm{FWHM})^2\rangle\approx 16\ln(2)\Delta E_0 k_B T_s = 16\ln(2)g_{\mathrm{TA}}(\theta)E_i k_B T_s. \quad (12)$$

For large scattering angles θ such as in the surface backscattering experiments discussed here, the narrowing of the intensity peak by the energy dependence of ΔE_0 can be quite significant and the TA may be a poor approximation.[24]

Equation (7) is the expected value of the FWHM for small v_R and exclusive of the effects of the form factor $|\tau_{fi}|^2$, which further narrows the width of the TOF distribution. When v_R is large and the term in $\Delta \mathbf{K}^2$ becomes important, the energy and temperature dependence of the FWHM is nearly the same as for Eq. (7), but the function $g(\theta)$ becomes smaller than the expression given in Eq. (10). Thus Eq. (7) can be regarded as a functional form with which to compare the energy and temperature dependence of the widths of the TOF spectra.

The analysis of the D_2 data is more complicated. Only a few theoretical models are in fact available to describe the scattering of symmetric diatomic molecules with a dynamic surface.[25,26] These models suggest that rotational excitation can be quite efficiently coupled with phonons[26] and that the coupling with phonons and electron–hole pair excitation can favor dissociative chemisorption.[25] Due to the sparsity of these theoretical investigations, Eq. (2) and the full quantum theory illustrated in Ref. 14 will be used throughout this paper to analyze the TOF distributions obtained with *both* He and D_2 scattering. The D_2 TOF distributions can, in fact, be regarded as the sum of two components. One component is represented by the D_2 molecules which exchange energy with the surface but do not change their rotational state when interacting with the surface. The energy distribution of this fraction of the molecules is expected to be similar to that of He atoms and should be correctly reproduced by Eq. (2). The second component is represented by the D_2 molecules which exchange energy with the surface and also change their rotational level. The energy distribution of these molecules is expected to deviate from the distribution predicted by theories developed for atomic scattering. Previous experimental studies of the scattering of NO molecules from metallic surfaces have shown that the scattered velocity distributions are rather insensitive to the final rotational state.[27,28] The ''pseudo-atomic'' theoretical approach illustrated in this section is therefore expected to hold also for the rotationally inelastically scattered molecules, at least to a first approximation. The extent to which Eq. (2) can account for the D_2 scattering data will give a measure of the role played by rotations in the scattering process.

III. EXPERIMENT

The experiments were carried out with a high-resolution He atom time-of-flight spectrometer developed for measuring surface phonon dispersion curves and described previously.[29] The incident beam strikes the target after passing through three differentially pumped chambers, one of which contains the chopper for time-of-flight measurements. After scattering at a fixed angle of $\theta_{SD}=95.76°$ with respect to the incident beam the particles are detected by a homemade electron bombardment magnetic mass spectrometer detector which has been optimized for high sensitivity and is located at a distance of 1.4 m from the target. The Cu crystal was oriented to within 0.5° and cleaned *in situ* by ion sputtering and annealing[12] until the carbon and sulfur surface contamination was found to be less than 0.5% of a monolayer by the Auger spectrometer. The target chamber had a base pressure of $\sim 4\times 10^{-11}$ mbar. The observation, at small incident energies and surface temperatures, of sharp He and D_2 diffraction peaks with a typical half-width of 0.35° indicates an atomically clean surface with order over distances of about 200 Å.

During the D_2 scattering experiments at surface temperatures $T_s<400$ K the crystal was periodically heated to a temperature $T_s=600$ K to avoid build-up of D atoms due to dissociative chemisorption of D_2 at the surface.

For the high-incident beam energies used in this experiment, $100\leqslant E_i\leqslant 250$ meV, a supersonic nozzle beam source was employed. This source consists of a sapphire tube with an orifice of diameter $d=74$ μm. The tube was heated by electron bombardment up to temperatures $T_0\sim 1300$ K. A four-layer tantalum radiation shield was mounted around the sapphire tube to reduce power dissipation to about 50 W at the higher source temperatures ($T_0>1000$ K). The radiation shield was kept at a negative potential with respect to the emitting filament to prevent electrons from reaching the D_2 beam. Due to limitations in the pumping speed of the nozzle chamber the nozzle was operated with pressures $P_0\leqslant 15$ bar. The source pressure P_0 was varied during the measurements to keep the incident flux constant. Measurements of the pressure increase in the nozzle and target chambers confirmed that the incident beam flux was constant to within 20%. This allows a direct comparison between the TOF spectra taken with different gases and at different incident energies reported below in Sec. IV.

The beam speed ratios S for He and D_2 varied between 13 and 30 as discussed in Ref. 30. These values of the speed ratio correspond to an energy resolution $\Delta E/E$ between 11% and 25%, which corresponds to an intrinsic beam full width at half-maximum (FWHM) of about 11 meV at $E_i=100$ meV and of about 60 meV at $E_i=250$ meV. To determine the influence of the intrinsic energy spread of the incident beam on the measured TOF distribution we employ the following relation valid for the widths of convoluted Gaussian peak shapes:

$$\mathrm{FWHM}_{\mathrm{exp}}^2=\mathrm{FWHM}_{\mathrm{multi}}^2+\mathrm{FWHM}_{\mathrm{beam}}^2, \tag{13}$$

which relates the experimentally measured values of the measured widths ($\mathrm{FWHM}_{\mathrm{exp}}$) to the intrinsic beam resolution ($\mathrm{FWHM}_{\mathrm{beam}}$) and the broadening due to the multiphonon interaction ($\mathrm{FWHM}_{\mathrm{multi}}$). The measured values of $\mathrm{FWHM}_{\mathrm{exp}}$ vary from a value of about 26 meV at $E_i=100$ meV and $T_s=100$ K to a value of about 90 meV at $E_i=250$ meV and $T_s\geqslant 550$ K. By using Eq. (13) the contribution of the incident beam energy spread $\mathrm{FWHM}_{\mathrm{beam}}$ to the experimental values $\mathrm{FWHM}_{\mathrm{exp}}$ is calculated to be less than 15% for most incident energies and surface temperatures considered by this experiment. The $\mathrm{FWHM}_{\mathrm{beam}}$ could be therefore safely ignored in the analysis of the TOF spectra.

A number of previous investigations[31–35] have demonstrated that the rotational populations of highly expanded supersonic molecular beams follow a nearly Boltzmann distribution (at least for the lowest rotational states) which is

TABLE I. Relative populations (in %) of the rotational levels j for D_2 nozzle beams for source conditions P_0d and incident beam energies E_i calculated with the empirical method described in Ref. 35.

E_i (meV)	P_0d (Torr cm)	T_R (K)	$j=0$	$j=1$	$j=2$	$j=3$	$j=4$
105	17.0	138	37.6	29.9	28.7	3.0	0.6
139	17.0	235	23.0	23.6	38.5	8.8	5.3
170	19.2	302	18.2	20.3	38.7	11.3	9.4
206	22.5	346	16.0	18.5	37.9	12.4	11.9
222	28.1	349	15.9	18.4	37.8	12.5	12.0
251	28.1	409	13.7	16.5	36.3	13.4	14.9

characterized by an effective rotational temperature T_R. In Ref. 35 an empirical method is described to estimate the value of T_R for a given value of the parameter P_0d and of the incident energy E_i. Table I reports the estimated rotational populations of the D_2 beam for the incident energies employed in this experiment. Because of the large spacing between the vibrational levels of the D_2 molecule[36] the occupation of the excited vibrational states is always below 1.3% for incident energies $E_i \leqslant 250$ meV.[30] The vibrational excitation of the D_2 molecules was therefore ignored in the analysis of the scattering data.

IV. EXPERIMENTAL RESULTS

Figure 1 shows a series of TOF spectra for He and D_2 scattered from the [100] direction of the Cu(001) surface. The surface temperature was $T_s=950$ K and the deviation angle $\Delta\theta=-3°$. In this notation the incident angle is given by $\theta_i=\theta_{SD}/2+\Delta\theta$ (see also Ref. 12). The energy was increased stepwise from a value $E_i\sim100$ meV to $E_i\sim250$ meV for both He and D_2 scattering. The intensities of the He TOF spectra are a factor 5 to 7 larger than those of D_2 for incident energies up to 210 meV. For incident energies $E_i>210$ meV the difference reduces to about a factor of 3. The D_2 TOF spectra taken at at energies $E_i=206$ meV and $E_i=222$ meV, respectively, are anomalous because they nearly coincide with a rotationally inelastic diffraction (RID) peak.[37] The RID peaks are diffraction peaks where the incident molecules convert a part of their translational energy into rotational energy. The position of the RID peaks is given by the equations for the conservation of parallel momentum and energy.[37]

$$\Delta\mathbf{K}=\mathbf{K}_f-\mathbf{K}_i=\mathbf{G},\qquad E_f-E_i=\Delta E_{\rm rot}, \tag{14}$$

where $\mathbf{G}$ is a surface reciprocal lattice vector, E_f and E_i are the final and incident beam energies, and $\Delta E_{\rm rot}$ is the rotational excitation energy. Values of $\Delta E_{\rm rot}$ for the transitions between the lowest rotational levels of the D_2 molecule can be found in Ref. 36. In the case of the TOF spectra taken at $E_i=206$ meV and $E_i=222$ meV the RID peak coupled with the rotational transition $j=3\rightarrow1$ ($\Delta E_{\rm rot}=36.88$ meV) and the vector $\mathbf{G}=(11)$ is located at an angular position of $\Delta\theta=-2.7°$. The conversion between rotational and translational energy increases the final translational energy of the D_2 molecules and explains the shift of the maximum of the TOF distributions towards positive values of the energy

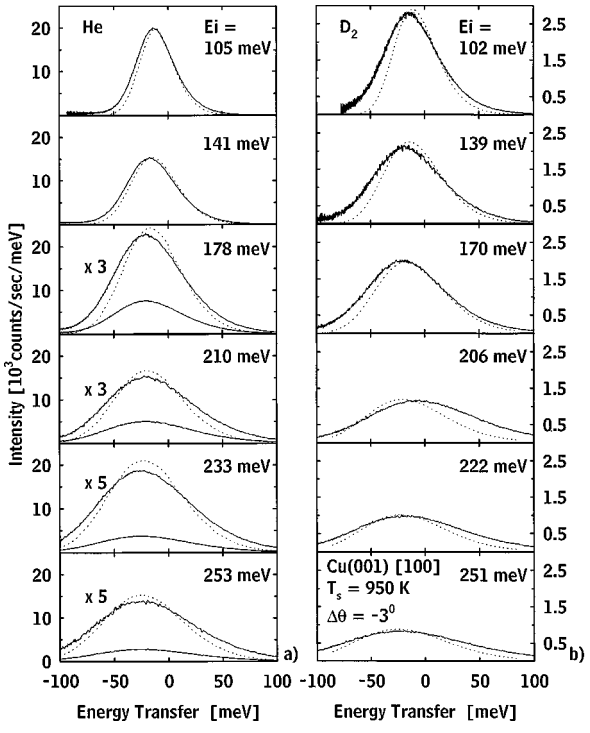

FIG. 1. Time-of-flight spectra of He (a) and D_2 (b) scattered from the [100] direction of Cu(001) at a temperature $T_s=950$ K and a deviation angle $\Delta\theta=-3°$. The incident energy was increased from $E_i\sim100$ meV to $E_i\sim250$ meV for both He and D_2 scattering. The D_2 TOF spectra at energies $E_i=206$ meV and $E_i=222$ meV are anomalous because of the proximity of a RID peak. The dotted lines indicate the best fit of Eq. (2) to the TOF spectra with the parameters reported in Table II.

TABLE II. Dependence on incident energy of the interaction parameters Q_c and β for scattering of He and D_2 from Cu(001) in the multiphoton classical regime. The parameters were determined from best-fits of Eq. (2) to the experimental data of Fig. 1. The fit procedure was carried out by fixing the parameter v_R to the value $v_R=3000$ m/s (Ref. 4) and the potential well depth to $\epsilon=5.76$ meV for He and $\epsilon=32.5$ meV for D_2. The value of the classical turning point Z_0 was calculated from Eq. (15).

E_i (meV)	β (Å^{-1})	Q_c (Å^{-1})	Z_0 (Å^{-1})
	He		
20–100[a]	3.0	1.0	3.0
105	5.7	2.4	0.99
113[b]	5.7	2.4	0.99
141	6.1	2.8	0.77
178	7.5	3.4	0.64
210	8.4	3.8	0.58
233	9.0	3.9	0.59
253	10.0	4.1	0.59
	D_2		
102	8.7	7.0	0.17
139	9.5	8.6	0.13
171	10	9.0	0.12
206	11.6	12.0	0.08
222	12.2	9.3	0.14
251	12.8	9.8	0.13

[a]Determined in Ref. 12 by analyzing scattering of He from Cu(001) in the quantum regime ($E_i<100$ meV).

[b]Determined in Ref. 4 by analyzing scattering of He from Cu(001) in the region of transition between the quantum regime and the multiphonon classical regime ($E_i\sim100$ meV).

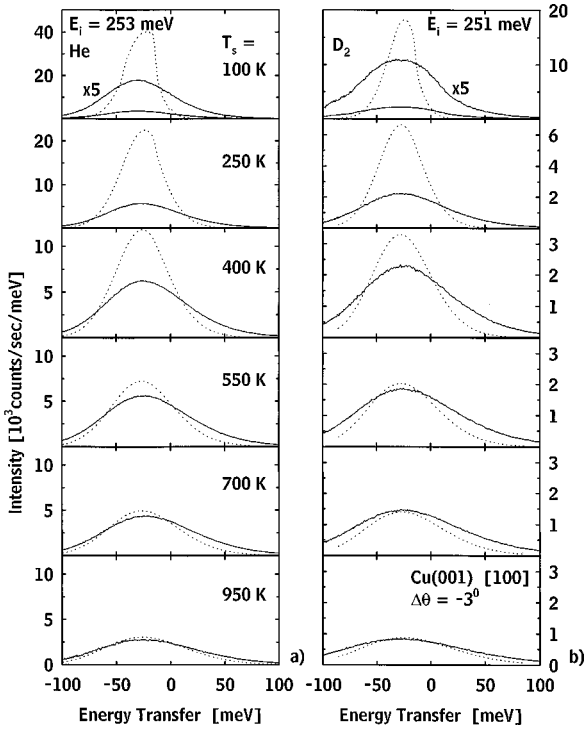

FIG. 2. Time-of-flight spectra of He (a) and D_2 (b) beams incident along the [100] direction of Cu(001). The beam energy was $E_i=253$ meV for He and $E_i=251$ meV for D_2, the deviation angle $\Delta\theta=-3°$. The surface temperature was varied from $T_s=100$ K to $T_s=950$ K. The dotted lines indicate the results of Eq. (2) when the parameters reported in Table II are used.

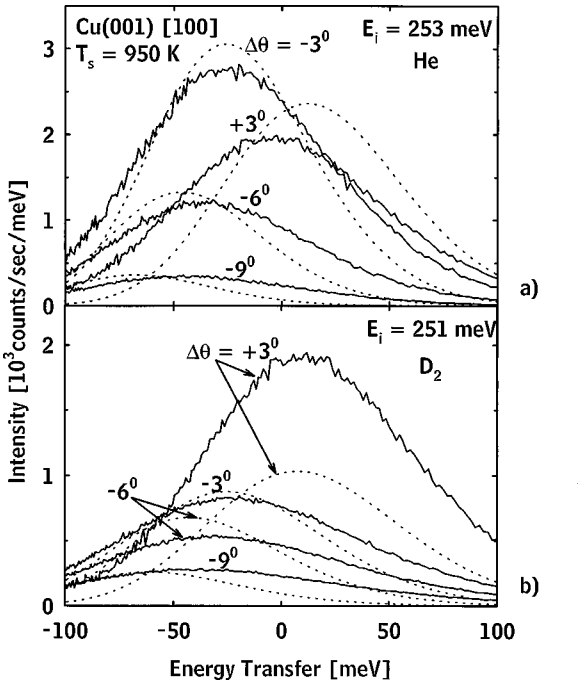

FIG. 3. Time-of-flight spectra of He and D_2 beams incident along the [100] direction of Cu(001). The surface temperature was $T_s=950$ K and the deviation angle was varied from $\Delta\theta=-9°$ to $\Delta\theta=3°$. (a) He measurements taken at $E_i=253$ meV; (b) D_2 measurements taken at $E_i=251$ meV. The dotted lines in (a) and (b) indicate the results of Eq. (2) when the parameters reported in Table II are used.

transfer ΔE. The dotted lines in Fig. 1 indicate the fit of Eq. (2) to the experimental data. The best-fit parameters are reported in Table II. It is important to notice that the form of the TOF distributions is a Gaussian-like profile for both He and D_2 scattering. Furthermore, the maximum intensity of the TOF distributions for a fixed incident energy is located at approximately the same value of the energy transfer for both He and D_2 scattering. These observations suggest that the mechanism of energy exchange with the surface is similar for He and D_2 and that rotational excitations do not play a predominant role.

Figure 2 shows a series of TOF spectra taken for He at an incident energy $E_i=253$ meV and for D_2 at an incident energy $E_i=251$ meV at a fixed deviation angle $\Delta\theta=-3°$. The surface temperature was increased from $T_s=100$ K to $T_s=950$ K. Similar to what is observed in Fig. 1 the intensities of the He TOF spectra are a factor 2 to 3 larger than those of D_2 over the whole range of surface temperatures. The dotted lines again indicate the results of Eq. (2) when the parameters reported in Table II are used.

Figure 3 shows a series of TOF spectra for He [Fig. 3(a)] and D_2 [Fig. 3(b)] beams scattered from the clean Cu(001) surface along the [100] direction at incident energies $E_i=253$ meV and $E_i=251$ meV, respectively. The surface temperature was $T_s=950$ K. The deviation angle was varied stepwise from $\Delta\theta=-9°$ to $\Delta\theta=3°$. The He and D_2 TOF spectra [Fig. 3(a)] display a falloff of the intensity when the crystal is rotated away from the specular direction by $\Delta\theta$. The D_2 TOF spectra [Fig. 3(b)] are about two to three times less intense than the corresponding He spectra, with the exception of $\Delta\theta=+3°$, and show a similar falloff of the intensity when the crystal is moved away from the specular position. The intensity of the D_2 TOF spectrum taken at an angle $\Delta\theta=3°$ is more than a factor of 2 higher than that of the other D_2 TOF spectra. This anomalously large intensity is probably due to the fact that the angular position at which this TOF spectrum was taken nearly coincides with that of the RID peak ($\Delta\theta=2.9°$) coupled to the transition $j=4\rightarrow2$ ($\Delta E_{\mathrm{rot}}=51.41$ meV) and the vector $\mathbf{G}=(00)$. The dotted lines indicate the results of Eq. (2) when the parameters reported in Table II are used.

Figure 4 displays as a function of surface temperature the maximum peak intensities (the intensity at the position of most probable energy transfer) of the He and D_2 TOF spectra taken at a fixed deviation angle $\Delta\theta=-3°$. In Ref. 4 it was shown in fact that the maximum peak intensity is an excellent parameter to characterize multiphonon scattering. For He scattering the data points follow the same trend for each incident energy. At low temperatures the intensity of the TOF spectra is low. The multiphonon scattering probability increases with surface temperature, reaches a maximum between 400 and 500 K, and decreases at higher surface temperatures. The physical reason for this behavior is the following. At low temperatures, when most of the scattering is in the quantum elastic and single-phonon inelastic peaks, the multiphonon intensity grows with increasing temperature at the expense of the intensity of the quantum peaks. At sufficiently high temperatures the quantum peaks become vanishingly small and virtually all of the intensity is in the classical multiphonon contribution and the multiphonon peak reaches

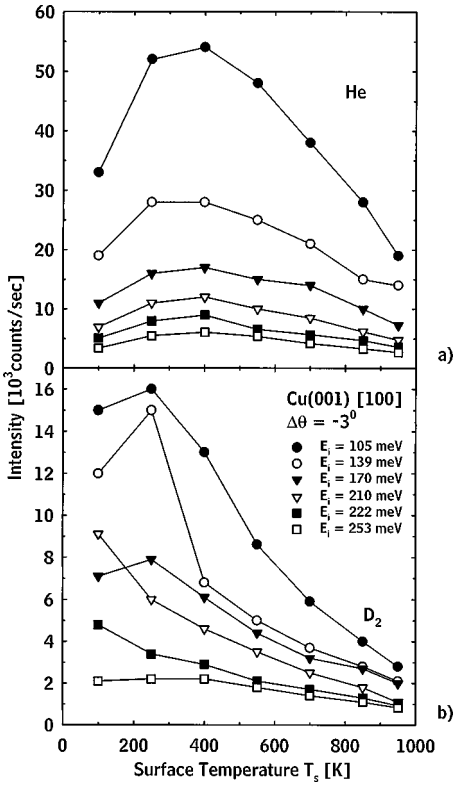

FIG. 4. Maximum peak intensities of time-of-flight spectra of He (a) and D_2 (b) beams incident along the [100] direction of Cu(001). In each data set the incident energy E_i is constant and the surface temperature T_s increases. The deviation angle was $\Delta\theta=-3°$. The lines are a guide to the eye.

a maximum. At still higher temperatures the multiphonon peak becomes broader by spreading out to larger energy exchanges and larger scattering angles, and, to conserve unitarity, the maximum peak intensity decreases. The analysis of the D_2 experimental data is complicated by the neighborhood of RID peaks at $E_i=210$ meV and $E_i=222$ meV. Except for the latter energies the maximum peak intensities of the D_2 TOF distributions raise to a maximum and then decrease more rapidly than in the case of He scattering.

Figure 5 displays as a function of incident energy the maximum peak intensities of the He and D_2 TOF spectra taken at a fixed deviation angle $\Delta\theta=-3°$. The data displayed in Fig. 5 are the same as in Fig. 4 but are now plotted as a function of energy rather than T_s. For He scattering, at each temperature T_s the maximum multiphonon excitation probability decreases by more than a factor of 5 when the incident energy changes from $E_i=105$ meV to $E_i=253$ meV. Figure 5(b) shows that for D_2 scattering the intensities decrease by only about a factor of 3 when the energy is varied over the same interval.

Figure 6 displays as a function of surface temperature the squares of the full widths at half maximum $(\mathrm{FWHM})^2$ of the He and D_2 TOF spectra taken at a fixed deviation angle $\Delta\theta=-3°$. The values of the FWHM were determined by Gaussian fits to the measured TOF distributions. For the same incident energy and surface temperature the values of the FWHM^2 for D_2 are about 15% larger than those of He. The solid lines indicate linear fits to the experimental data. The anomalous slopes of the D_2 scattering data taken at the

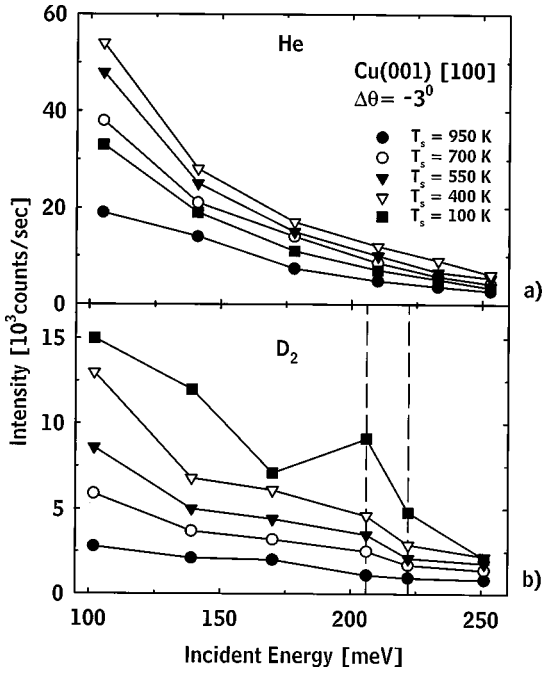

FIG. 5. Maximum peak intensities of time-of-flight spectra of He (a) and D_2 (b) beams incident along the [100] direction of Cu(001). In each data set the surface temperature T_s is constant and the incident energy E_i increases. The deviation angle was $\Delta\theta=-3°$. The lines are a guide to the eye. The vertical dashed lines in (b) indicate the energies where a RID peak is in the immediate neighborhood of $\Delta\theta=-3°$.

incident energies $E_i=210$ meV and $E_i=222$ meV are exceptions due to the proximity of RID peaks as reported in the discussion of Fig. 1.

V. DISCUSSION

A. Energy dependence

To clarify the dependence of the multiphonon excitation probability on incident energy Eq. (2) was fitted to the ex-

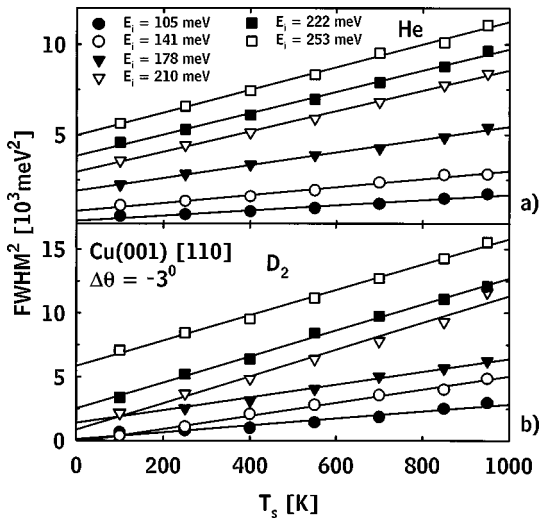

FIG. 6. The FWHM^2 of time-of-flight spectra of He (a) and D_2 (b) beams incident along the [100] direction of Cu(001). In each data set the incident energy is constant and the surface temperature T_s increases. The deviation angle was $\Delta\theta=-3°$. The solid lines are linear fits to the experimental data. The slope of the best-fit lines to the D_2 data taken at $E_i=210$ meV and $E_i=222$ meV are anomalous due to the proximity of RID peaks.

perimental data of Fig. 1. The measurements of Fig. 1 were taken at incident energies and surface temperatures which fulfill the condition $2W>6$ and therefore Eq. (2) is expected to be a reasonable approximation. The fit of Eq. (2) to the experimental data was carried out by keeping the value of the velocity parameter constant at $v_R=3000$ m/s determined in Refs. 4 and 5. Here v_R is expected to have a value comparable to the velocity of the Rayleigh wave on Cu(001) (which is 1700 m/s)[12] and is not expected to depend strongly on incident energy. The results of the fit procedure were checked separately using Eq. (2) with the parameters of Table II to reproduce a series of TOF spectra where the deviation angle $\Delta\theta$ was varied. The results of the theoretical calculations are reported in Fig. 3 and show a substantial agreement with experiment, which confirms the validity of the chosen theoretical approach and of the best-fit parameters.

The best-fit values of Q_c and β for He scattering increase with incident energy. The increase of the cutoff parameter Q_c with incident energy is expected. Here Q_c expresses the range of the interaction between the incident particles and the surface.[20] At high incident energies, the incident projectiles come closer to the surface and the interaction with the surface becomes increasingly short ranged, which results in a larger value of Q_c. The increase of the parameter β with incident energy expresses an increase in stiffness of the repulsion potential, which reflects probably an increase in strength of the Pauli repulsion when the atoms come closer to the surface.

The values of β and Q_c are related to each other, and an approximate expression of this relation is[22]

$$Z_0=\frac{\beta}{Q_c^2}, \tag{15}$$

where Z_0 is the classical turning point. The approximations used for obtaining Eq. (15) are sufficiently crude that one does not expect quantitative agreement. The values of Z_0 obtained from Eq. (15) using the best-fit values of Q_c and β are reported in Table II. The turning point is located at $Z_0=0.99$ Å for an incident energy $E_i=105$ meV and coincides with the value determined in Refs. 4 and 5 also with an analysis of He multiphonon scattering from Cu(001). The value $Z_0=0.99$ Å determined for an energy $E_i=105$ meV is about a factor of 3 less than the value $Z_0=3.0$ Å determined from single-phonon measurements in Ref. 12, and of the value $Z_0=3.48$ Å which can be determined for an energy $E_i=100$ meV from the He/Cu(001) potential energy diagram reported in Ref. 15. This discrepancy is probably due to the crude approximations which are made in the derivation of Eq. (15), and it is probably more appropriate to regard the values of Z_0 reported in Table II as effective values. The variation $\Delta Z_0=0.4$ Å determined from the best-fit parameters is, however, in good agreement with the value $\Delta Z_0\sim 0.3$ Å which can be calculated for the energy range $100\leqslant E_i\leqslant 250$ meV from the He/Cu(001) potential energy diagram determined by very recent work.[15] Recent calculations of Petersen *et al.* show also a variation $\Delta Z_0\sim 0.3$ Å for He on Rh(110) when the incident energy changes from $E_i=100$ meV to $E_i=200$ meV.[38]

Turning to molecular scattering, the similar form of the TOF distributions obtained for He and D_2 scattering (Figs. 1–3) is a strong indication that the rotational degree of freedom does not play a predominant role in determining the energy exchange with the surface. For this reason, a systematic fit of Eq. (2) to the data of Fig. 1 is reasonable even in the case of D_2 scattering.

The best-fit values of Q_c and β for D_2 scattering increase with incident energy much like in the case of He scattering. The best-fit values of Q_c are a factor of 2.5 to 3 higher than those of He for the same incident energy, which would indicate that the D_2 molecules have a much more localized interaction with the surface than the He atoms. This aspect probably reflects the different position of the minimum of the physisorption potential which is located at $z_p\sim 3.6$ Å for D_2 (Refs. 39 and 40) and at $z_p\sim 4.2$ Å for He.[15] The best fit values of β determined for D_2 scattering are a factor of 1.3 to 1.5 greater than the values for He scattering for similar incident energies. This behavior is somewhat unexpected. Previous studies of the physisorption potential have shown in fact that at least at energies $E_i\leqslant 30$ meV the repulsion parameter is similar, $\beta\sim 2.43$ Å^{-1} for He/Cu(001) (Ref. 16) and $\beta\sim 2.28$ Å^{-1} for D_2/Cu(001).[39,40] Comparisons of diffraction experiments with theoretical models yield also a value $\beta=2.1$ Å^{-1} for He scattering from the close packed surfaces of Cu.[41,42] Further, the classical turning point Z_0 calculated for D_2 from Eq. (15) with the best-fit values is weakly dependent on incident energy. These differences between the best-fit parameters for He and D_2 scattering may be due to the rotational transitions of D_2 molecules, which are not taken into account by the multiphonon scattering theory described in Sec. II.

B. Temperature dependence

Figures 2 and 4 illustrate the temperature dependence of the multiphonon excitation probability. In Fig. 2 the dotted lines indicate the results of Eq. (2) when the parameters reported in Table II are used and the surface temperature is varied. The theoretical predictions for both He and D_2 are in good agreement with the experimental data for temperatures $T_s\geqslant 550$ K but overestimate the multiphonon scattering probability at low temperatures where the semiclassical theory of Eq. (2) is not a good approximation. A similar but less pronounced discrepancy between theory and experiment at low surface temperatures was reported also in Refs. 4 and 5 even in the case of the full quantum calculations and is probably due to an inadequate theoretical description of the transition between quantum and multiphonon classical regime. The value of the Debye–Waller exponent is in fact $2W\sim 3$ for He scattering at an incident energy $E_i=253$ meV and a surface temperature $T_s=100$ K. Under these conditions Eq. (2) is not valid. For D_2 scattering, the Debye–Waller exponent is $2W\sim 7$ for an incident energy $E_i=251$ meV and a surface temperature $T_s=100$ K, and the discrepancy between theory and experiment is less marked than in the case of He. The exact determination of the multiphonon scattering probability as a function of surface temperature constitutes at the present stage one of the challenging aspects of the theoretical interpretation.[4,5]

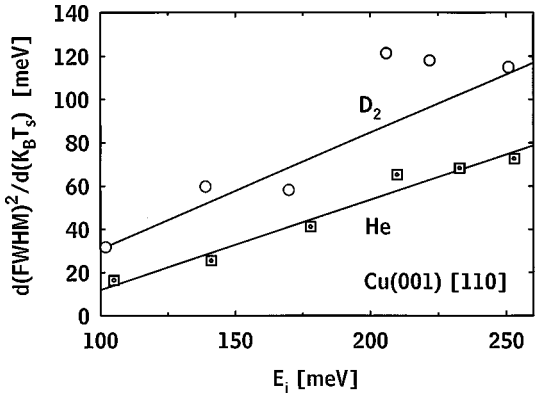

FIG. 7. The slope of the squared widths $d(\mathrm{FWHM})^2/d(k_BT_s)$ as a function of incident energy. Dotted squares: He. Circles: D_2. The lines are linear fits to the data. The D_2 data taken at an energy $E_i=206$ meV and $E_i=222$ meV are anomalous because of the proximity of RID peaks and were not considered in the linear fit.

C. FWHM of the TOF spectra

Equation (7) shows that in the classical multiphonon regime the squares of the measured values of the FWHM of the TOF spectra depend linearly on incident energy and surface temperature. The linear dependence on surface temperature is clearly demonstrated by the data reported in Fig. 6. Since furthermore the derivative of Eq. (7) with respect to temperature is

$$\frac{d(\mathrm{FWHM})^2}{k_{\mathrm{B}}\,dT_s}=16\ln(2)g(\theta)E_i, \tag{16}$$

then the slopes of the best-fit lines to the data of Fig. 6 are expected to depend linearly on incident energy. In Fig. 7 a plot of the slopes as a function of incident energy is reported. The data, with the exception of those D_2 points associated with RID, lie rather well on straight lines and confirm that Eq. (7) gives the correct functional dependence of the FWHMs on incident energy and surface temperature for both He and D_2 scattering. Table III reports the slopes of the best-fit lines to the data of Fig. 7, as well as the values of the slopes calculated from Eq. (2) and from the idealized expression of Eq. (7). Note that Eq. (7) gives a reasonable functional form for the energy and temperature dependence, but it does not account for the additional narrowing of the FWHM by the form factor $|\tau_{fi}|^2$ or by the correlation effects of the weighted average parallel phonon velocity v_R in Eq. (2).

Table III shows that the agreements of the double slope $d^2(\mathrm{FWHM}^2)/d(k_{\mathrm{B}}T_s)d(E_i)$ with the full calculations using Eq. (2) are rather good, as can be expected from the theoretical fits shown in Figs. 1 and 2. The experimental value of the dimensionless double slope for D_2 is 0.54, which is about 20% larger than the value of 0.42 for He. The fact that the values calculated directly from Eq. (2) also reflect this difference is due to the difference in choices of the parameters β and Q_c for D_2 and He, and this in turn indicates that the potential is stiffer and shorter ranged for D_2. However, it should be noted that the effects of the physisorption well in the potential are not included in the calculation of ΔE_0 using Eq. (2). In the simplest approximation of assuming that the potential well simply increases the speed of the particle before colliding with the repulsive surface (the Beeby correction), as discussed in connection with Eq. (1), one would expect that because this makes $2W$ larger and hence also makes ΔE_0 larger, the potential well would enhance the value of the slope. This enhancement would be greater for D_2 because of its larger well depth, in qualitative agreement with the present observations.

TABLE III. Experimental and theoretical values of the dimensionless energy and temperature slopes of the squared peak widths, $d^2(\mathrm{FWHM}^2)/d(k_BT_s)d(E_i)$. The experimental values are from the data of Fig. 7. The calculated values are from the calculations shown in Figs. 1 and 2. The value obtained from Eq. (7) represents a theoretical upper limit.

	Experimental	Calculation	Eq. (7)
He	0.418 ± 0.037	0.381 ± 0.015	1.066
D_2	0.538 ± 0.086	0.498 ± 0.009	1.066

This work shows that the energy and temperature dependence of the TOF spectra can be reasonably explained by the theory reported in Sec. II. There are significant differences between He and D_2 scattering which can be ascribed to rotational transitions in D_2, and there are strong indications that the differences of the physisorption potential, the range of the projectile–surface interaction, and the steepness of the repulsion potential must be taken into account. The probability of rotationally inelastic transitions does not appear to depend on surface temperature and indicates a weak coupling between phonon excitation and rotational transitions, in qualitative agreement with previous experimental results.[27,28]

This investigation demonstrates that the shapes and intensities of the He and D_2 TOF spectra can be accounted for quite well by a multiphonon scattering theory developed for the atomic scattering case[14] when the differences in the physisorption potential of He and D_2 are taken into consideration.

ACKNOWLEDGMENTS

The authors would like to thank J. P. Toennies for helpful discussions during the course of this work. J.R.M. was supported by the NSF under Grant No. DMR-9726229. M.F.B. was supported by the ''Training and Mobility of Researchers'' program of the European Union (Grant No. ERBFMBICT950377).

[1] J. A. Barker and D. J. Auerbach, Surf. Sci. Rep. **4**, 1 (1984).
[2] A. Bilic and B. Gumhalter, VUOTO, Sci. Tech. **24/1**, 13 (1995).
[3] A. Bilic and B. Gumhalter, Phys. Rev. B **52**, 12 307 (1995).
[4] F. Hofmann, J. R. Manson, and J. P. Toennies, Surf. Sci. **349**, L184 (1996).
[5] F. Hofmann, J. R. Manson, and J. P. Toennies, J. Chem. Phys. **106**, 1234 (1997).
[6] G. G. Bishop, W. P. Brug, G. Chern, J. Duan, S. A. Safron, and J. G. Skofronick, Phys. Rev. B **47**, 3966 (1993).
[7] V. Celli, D. Himes, P. Tran, J. P. Toennies, Ch. Wöll, and G. Zhang, Phys. Rev. Lett. **66**, 3160 (1991).
[8] J. R. Manson, Phys. Rev. B **43**, 6924 (1991).
[9] J. R. Manson, Surf. Sci. **272**, 130 (1992).
[10] J. R. Manson and J. G. Skofronick, Phys. Rev. B **47**, 12890 (1993).

[11] A. Muis and J. R. Manson, Phys. Rev. B **53**, 2205 (1996).
[12] F. Hofmann, J. R. Manson, and J. P. Toennies, J. Chem. Phys. **101**, 10155 (1994).
[13] J. L. Beeby, J. Phys. C **4**, L359 (1971).
[14] J. R. Manson, Comput. Phys. Commun. **80**, 145 (1994).
[15] J. Ellis, K. Hermann, F. Hofmann, and J. P. Toennies, Phys. Rev. Lett. **75**, 886 (1995).
[16] E. Zaremba and W. Kohn, Phys. Rev. B **13**, 2270 (1976).
[17] G. Benedek, M. F. Bertino, S. Miret-Artes, and J. P. Toennies, Surf. Sci (accepted).
[18] R. Brako and D. M. Newns, Phys. Rev. Lett. **48**, 1859 (1982).
[19] F. O. Goodman and A. Y. Wachman, in *Dynamics of Gas-Surface Scattering* (Academic, New York, 1972), Chap. 8.
[20] V. Celli, in *Helium Atom Scattering from Surfaces*, edited by E. Hulpke (Springer, Berlin, 1992), pp. 25–40.
[21] R. B. Doak, in *Atomic and Molecular Beam Methods*, edited by G. Scoles (Oxford University Press, Oxford, 1988), Vol. II, pp. 323–360.
[22] V. Celli, G. Benedek, U. Harten, J. P. Toennies, R. B. Doak, and V. Bortolani, Surf. Sci. **143**, L376 (1984).
[23] A. Sjölander, Ark. Fys. **14**, 315 (1959).
[24] C. A. DiRubio, D. M. Goodstein, B. H. Cooper, and K. Burke, Phys. Rev. Lett. **73**, 2768 (1994).
[25] G. Billing, J. Phys. Chem. **99**, 15378 (1995).
[26] A. J. Cruz and B. Jackson, J. Phys. Chem. **91**, 4985 (1989).
[27] J. Kimman, C. T. Rettner, D. J. Auerbach, J. A. Barker, and J. C. Tullym, Phys. Rev. Lett. **57**, 2053 (1996).
[28] C. T. Rettner, J. Kimman, and D. J. Auerbach, J. Chem. Phys. **94**, 734 (1991).
[29] J. P. Toennies, in *Surface Phonons*, edited by W. Kress and F. W. de Wette (Springer, Berlin, 1991), pp. 111–166.
[30] M. F. Bertino, A. P. Graham, L. Yu Rusin, and J. P. Toennies, in preparation.
[31] D. R. Miller, in *Atomic and Molecular Beam Methods*, edited by G. Scoles (Oxford University Press, Oxford, 1988), Vol. I, pp. 14–53.
[32] K. Winkelmann, *11th International Symposium on Rarefied Gas Dynamics*, edited by R. Campargue (Commissariat a l'Energie Atomique, Paris, 1979), p. 899.
[33] J. E. Pollard, D. J. Trevor, Y. T. Lee, and D. A. Shirley, J. Chem. Phys. **77**, 4819 (1982).
[34] K. Kern, R. David, and G. Comsa, J. Chem. Phys. **82**, 5673 (1985).
[35] M. Faubel, F. A. Gianturco, F. Ragnetti, L. Y. Rusin, F. Sondermann, and U. Tappe, J. Chem. Phys. **101**, 8800 (1994).
[36] K. P. Huber and G. Herzberg, *Molecular Spectra and Molecular Structure* (Van Nostrand, New York, 1978), Vol. IV.
[37] M. F. Bertino, F. Hofmann, and J. P. Toennies, J. Chem. Phys. (accepted).
[38] M. Petersen, S. Wilke, P. Ruggerone, B. Kohler, and M. Scheffler, Phys. Rev. Lett. **76**, 995 (1996).
[39] P. Nordlander, C. Holmberg, and J. Harris, Surf. Sci. **152/153**, 702 (1985).
[40] L. Wilzen, F. Althoff, S. Andersson, and M. Persson, Phys. Rev. B **43**, 7003 (1991).
[41] J. Lapujoulade and J. Perreau, Surf. Sci. **122**, 341 (1982).
[42] G. Armand and J. R. Manson, J. Phys. (France) **44**, 473 (1983).